Dalton Transactions

An international journal of inorganic chemistry

www.rsc.org/dalton

Number 13 | 7 April 2008 | Pages 1649–1796

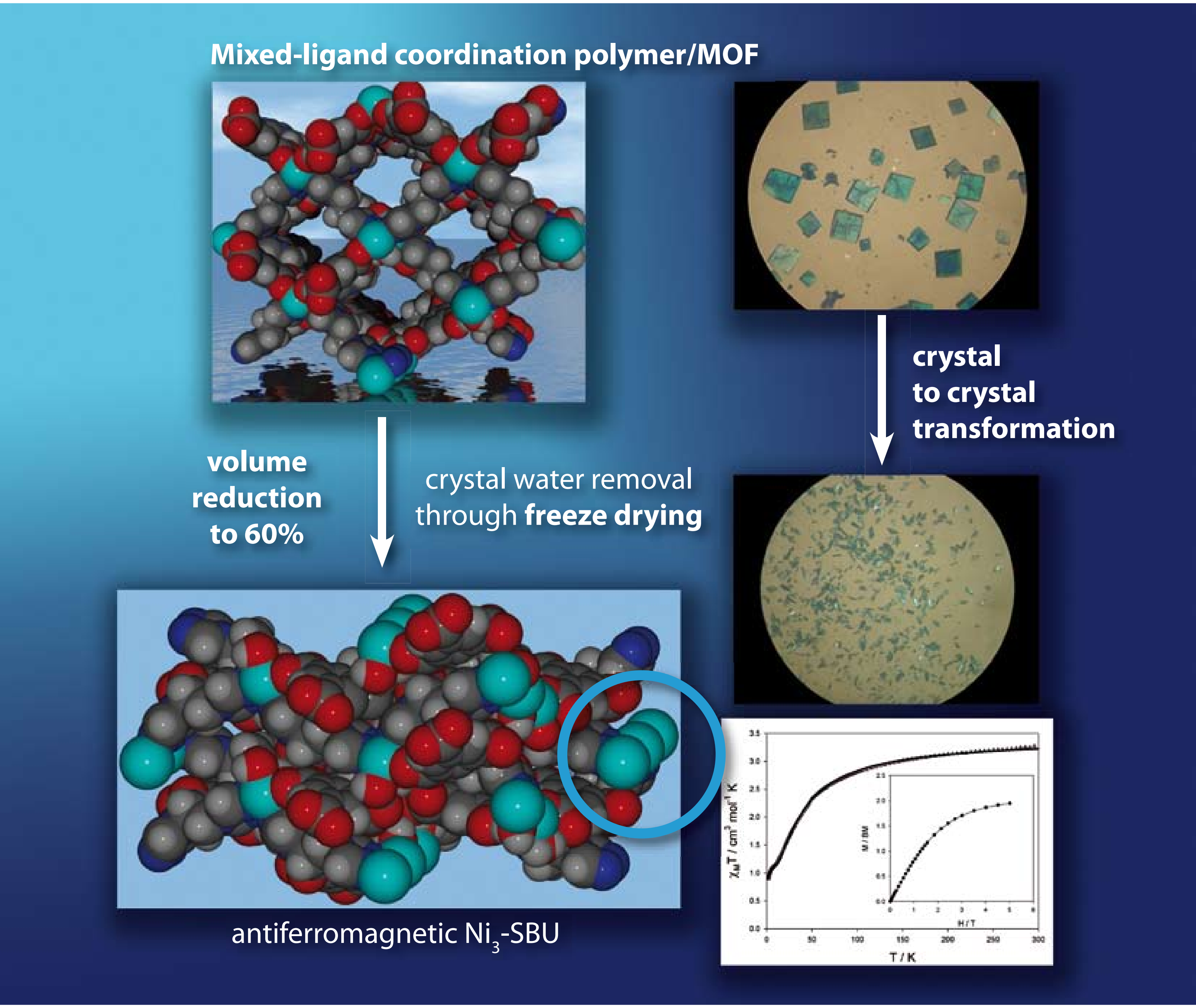

ISSN 1477-9226

RSC Publishing

HOT ARTICLE
Janiak *et al.*
Mixed-ligand coordination polymers from 1,2-bis(1,2,4-triazol-4-yl)ethane and benzene-1,3,5-tricarboxylate

PERSPECTIVE
Thompson *et al.*
Ligand directed self-assembly of polymetallic [$n \times n$] grids: rational routes to large functional molecular subunits?

1477-9226(2008)13;1-7

Mixed-ligand coordination polymers from 1,2-bis(1,2,4-triazol-4-yl)ethane and benzene-1,3,5-tricarboxylate: Trinuclear nickel or zinc secondary building units for three-dimensional networks with crystal-to-crystal transformation upon dehydration†

Hesham A. Habib,[a] Joaquin Sanchiz[b] and Christoph Janiak*[a]

Received 12th October 2007, Accepted 22nd January 2008
First published as an Advance Article on the web 27th February 2008
DOI: 10.1039/b715812b

The hydrothermal reaction of $M(NO_3)_2\cdot 6H_2O$ (M = Ni and Zn) with benzene-1,3,5-tricarboxylic acid (H_3btc) and 1,2-bis(1,2,4-triazol-4-yl)ethane (btre) produced the mixed-ligand coordination polymers (MOFs) ${}^3_\infty\{[Ni_3(\mu_3\text{-btc})_2(\mu_4\text{-btre})_2(\mu\text{-}H_2O)_2]\cdot\sim 22H_2O\}$ (**1**) and ${}^3_\infty\{[Zn_3(\mu_4\text{-btc})_2(\mu_4\text{-btre})(H_2O)_2]\cdot 2H_2O\}$ (**3**). The compounds, characterized by single-crystal X-ray diffraction, X-ray powder diffraction and thermoanalysis feature trinuclear secondary building units (SBU) within the three-dimensional frameworks. The trinuclear nickel unit in **1** exhibits an intra-trimer together with some weak inter-trimer antiferromagnetic coupling with $J = -13.88(8)\ \text{cm}^{-1}$ from the magnetic susceptibility measurement between 1.9–300 K. The zinc coordination polymer **3** shows a strong fluorescence at 423 nm upon excitation at 323 nm (not seen in the free btre ligand). Compound **3** is thermally robust until 200 °C (ambient pressure) where loss of the water molecules starts. Careful control of the dehydration procedure (freeze-drying) for **1** and (heating to 280 °C) for **3** allowed for a solid-state reaction with single-crystal-to-single-crystal structural transformations in obtaining the largely dehydrated products ${}^3_\infty\{[Ni_3(\mu_2\text{-btc})_2(\mu_4\text{-btre})_2(\mu\text{-}H_2O)_2(H_2O)_2]\cdot 4H_2O\}$ (**2**) and ${}^3_\infty\{[Zn_3(\mu_6\text{-btc})_2(\mu_4\text{-btre})_2]\cdot\sim 0.67H_2O\}$ (**4**), respectively. In the transformation from **1** to **2** the unit cell volume is reduced to about 60%. The transition from **3** to **4** involves breakage and formation of new Zn–O bonds.

Introduction

Metal–organic frameworks (MOFs) or coordination polymers have recently attracted much attention because of their topology and potential applications in catalysis, adsorption (gas storage), luminescence, magnetism, *etc.*[1–3] A key step for the construction of polymeric transition metal complexes is to select appropriate multidentate bridging ligands,[1,2,4] with mixed-ligand coordination polymers becoming more important recently.[5] Multi-carboxylic ligands with suitable spacers, especially benzoic acid-based ligands and also the 1,2,4-triazole ligand and its derivatives[6] are frequent choices for metal–organic networks.[1,2] Benzene-1,3,5-tricarboxylic acid (H_3btc, also known as trimesic acid) is a rigid, planar molecule and has been extensively used in the form of its three benzene-1,3,5-tricarboxylate anions $H_n\text{btc}^{(3-n)-}$ (n = 0, 1, 2) (Scheme 1) as a bridging ligand in the synthesis of multidimensional MOFs. Recent examples[7] (metals as cations and ligand bridging mode in parentheses) are for $H_2\text{btc}^-$ (Mn-μ_2),[8] for Hbtc^{2-} (Mn-μ_2,[9] Mn-μ_3,[9,10] Co-μ_2,[11] Co-μ_3,[9,10] Ni-μ_3,[12] Cu-μ_2,[13] Zn-μ_2,[9,10,14] Zn-μ_3 and -μ_4,[10] Cd-μ_3,[15]) and for btc^{3-}, (Fe-$\mu_{2,3}$,[16] Co-μ_2,[17] Co-μ_3,[18] Ni-μ_2,[17,19] Ni-μ_3,[20,21] Cu-$\mu_{2,3}$,[22], Cu-μ_3,[23] Zn-μ_3,[21,24] Ag-μ_3,[25] Ag-$\mu_{5,6}$,[26] In-μ_3,[27] Y-μ_2,[28]). The 1,2,4-triazole ligand and its 4-substituted derivatives can be used to obtain linear coordination polymers based on its bridging function, *e.g.* with Cu^{2+},[29] Zn^{2+},[30] Cd^{2+},[31] together with a wide variety of molecular polynuclear complexes.[32] The N1,N2-bridging mode of 1,2,4-triazole or triazolate (Scheme 1) constitutes a short ligand bridge between metal atoms which is a prerequisite for stronger magnetic

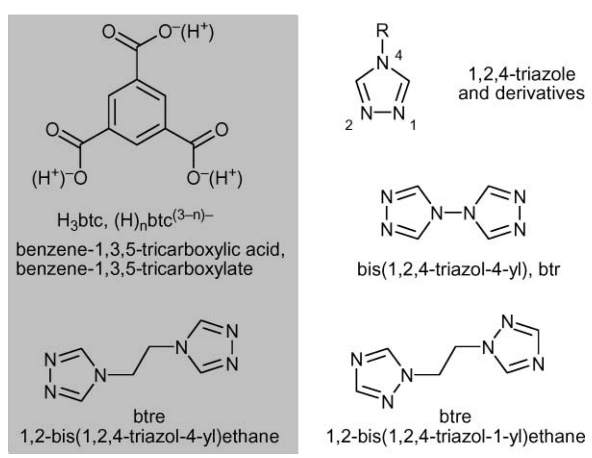

Scheme 1 Ligands relevant to this work. The gray underlined ligands btc and btre are synthetically used in this work.

[a]*Institut für Anorganische und Analytische Chemie, Universität Freiburg, Albertstr. 21, D-79104, Freiburg, Germany. E-mail: janiak@uni-freiburg.de; Fax: +49 761 2036147; Tel: +49 761 2036127*
[b]*Departamento de Química Inorganíca, Universidad de La Laguna, 38200, La Laguna, Tenerife, Spain*

† CCDC reference numbers [CCDC NUMBER(S)]. For crystallographic data in CIF or other electronic format see DOI: 10.1039/b715812b
Electronic supplementary information (ESI) available: X-Ray powder diffractograms; BET isotherms of a dried sample of **1**; hydrogen-bonding interactions; crystal data and structure refinement for thermally treated crystals of **3**. See DOI: 10.1039/b715812b

coupling between paramagnetic metal centers.[1] Surprisingly, with the related 4,4′-bis(1,2,4-triazol-4-yl) ligand (abbreviated as btr) this N1,N2 bridging coordination mode has only been observed recently with Cu(II).[7,33] Typically the btr ligand links transition metal(II) ions using only one nitrogen atom from each 1,2,4-triazole ring, resulting in one-,[34,35] two-, and three-dimensional[36–38] networks. When spacers, like methylene groups, are introduced between the two 1,2,4-triazole rings, the resulting ligand acquires more flexibility. Therefore we selected 1,2-bis(1,2,4-triazol-4-yl)ethane (abbreviated as btre). This btre ligand, which must not be mistaken with the 1,2-bis(1,2,4-triazol-*1*-yl)ethane ligand,[39] has been scarcely used in metal-complex or MOF synthesis. A CSD search[7] gave $^2_\infty\{M(NCS)_2(\mu_2\text{-btre-}\kappa N1,N1')_2(NCS)_2\}$ (M = Fe, Co)[40] and $^3_\infty\{[Cu_3(\mu_4\text{-btre-}\kappa N1,N2,N1',N2')_2(\mu_3\text{-btre-}\kappa N1,N2,N1')_4(H_2O)_2]_2(ClO_4)_{12}\cdot 2H_2O\}$ as the only examples. The Cu compound consists of trinuclear metal units interconnected by btre ligands with two different μ_3- and μ_4-bridging modes.[41]

In this work we report on the structures and properties of mixed-ligand coordination polymers with the btre ligand: $^3_\infty\{[Ni_3(\mu_3\text{-btc})_2(\mu_4\text{-btre})_2(\mu\text{-}H_2O)_2]\cdot{\sim}22H_2O\}$ (**1**), $^3_\infty\{[Ni_3(\mu_2\text{-btc})_2(\mu_4\text{-btre})_2(\mu\text{-}H_2O)_2(H_2O)_2]\cdot 4H_2O\}$ (**2**), $^3_\infty\{[Zn_3(\mu_4\text{-btc})_2(\mu_4\text{-btre})(H_2O)_2]\cdot 2H_2O\}$ (**3**) and $^3_\infty\{[Zn_3(\mu_6\text{-btc})_2(\mu_4\text{-btre})]\cdot 0.67H_2O\}$ (**4**) including the single-crystal-to-single-crystal transformations from **1** to **2** and **3** to **4**.

Results and discussion

Syntheses

Hydrothermal treatment of metal nitrates with 1,2-bis(1,2,4-triazol-4-yl)ethane (btre) and benzene-1,3,5-tricarboxylic acid (H_3btc) yields the mixed-ligand coordination polymers **1** or **3** (eqn (1)).

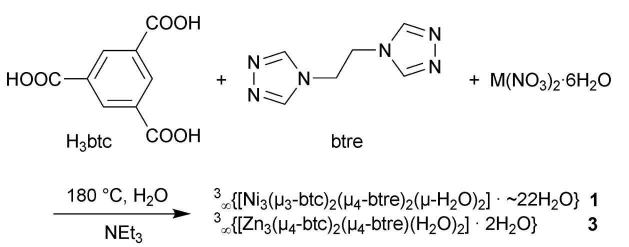

(1)

Complete deprotonation of H_3btc is achieved through the addition of triethylamine (NEt_3).

Thermal stability

Degradation of the organic parts of the mixed-ligand networks **1** and **3** starts above 300 °C according to thermogravimetric analyses (Scheme 2). Compound **1** easily loses part of its water of crystallization upon removal from the mother liquor. Drying of **1** in air yields a light blue substance which is somewhat amorphous by X-ray powder diffractometry. Further drying under vacuum (1.5 mbar, 6 h) gives a pale blue substance, which turns green when the drying temperature under vacuum is raised to 50 °C (6 h). Exposing the green substance to moist air returns the pale blue color. When **1** is quickly transferred from the water phase to the TGA capsule (without prolonged drying and vacuum conditioning) the first weight loss starts immediately and

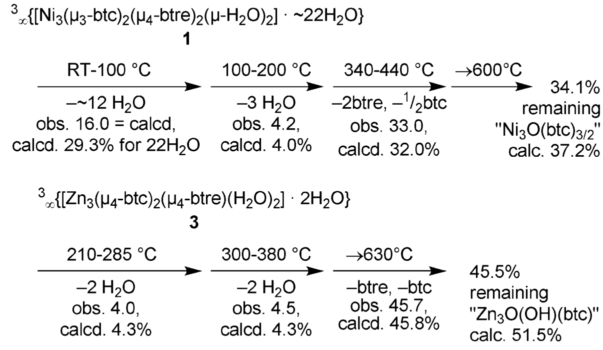

Scheme 2 Thermogravimetric analyses of **1** and **3**.

corresponds to the removal of the (remaining) water molecules of crystallization. Crystalline samples of **3** were dried at 35 °C and 1.5 mbar for 6 h and at 100 °C and 10^{-4} mbar (turbomolecular pump) for 6 h. No loss of crystallinity could be observed under the polarization microscope. X-Ray data sets were collected for single crystals from each of these dried samples. Structure solution and the quality of refinement was identical to the one from the unheated crystal probe (see ESI†), the crystal water was still present in the framework.

Crystal-to-crystal transformations

A crystalline sample of **1** was filtered off within 1 min in air, then freeze dried at −5 °C (ice bath with NaCl) and 10^{-4} mbar for 8 h. A blue-green crystalline product **2** was obtained (eqn (2))

solid-state crystal-to-crystal transformation:

$$\underset{\mathbf{1}}{^3_\infty\{[Ni_3(\mu_3\text{-btc})_2(\mu_4\text{-btre})_2(\mu\text{-}H_2O)_2]\cdot{\sim}22H_2O\}} \xrightarrow[-\,{\sim}16\,H_2O]{-5\,°C,\ 10^{-4}\,\text{mbar}} \underset{\mathbf{2}}{^3_\infty\{[Ni_3(\mu_2\text{-btc})_2(\mu_4\text{-btre})_2(\mu\text{-}H_2O)_2(H_2O)_2]\cdot 4H_2O\}} \quad (2)$$

which was stored at −20 °C under N_2 until investigated by single-crystal X-ray crystallography.

A crystalline sample of **3** was placed in a simultaneous thermoanalysis apparatus (STA 409 from Netzsch). The probe chamber was evacuated to 2 mbar and then refilled with N_2. After that the sample was heated to 280 °C with a heating rate of 10 K min^{-1} (eqn (3)).

solid-state crystal-to-crystal transformation:

$$\underset{\mathbf{3}}{^3_\infty\{[Zn_3(\mu_4\text{-btc})_2(\mu_4\text{-btre})_2(H_2O)_2]\cdot 2H_2O\}} \xrightarrow[-\,{\sim}3.3\,H_2O]{\text{RT-280 °C, 10 K/min}} \underset{\mathbf{4}}{^3_\infty\{[Zn_3(\mu_6\text{-btc})_2(\mu_4\text{-btre})_2]\cdot{\sim}0.67H_2O\}} \quad (3)$$

The still crystalline product **4** was transferred directly to the X-ray diffractometer.

Careful control of the evacuation or heating procedure allowed the largely dehydrated products **2** and **4** to be obtained as single-crystals, suitable for X-ray diffraction. Both transformations from **1** to **2** and from **3** to **4** represent rare cases of solid-state reactions with crystal-to-crystal transformations.[42] The almost complete dehydrations appear to be irreversible transformations.

The vibrational modes for carboxylate groups, substituted benzene and triazole rings confirm the presence of btc and btre ligands in **1** and **3**. The absence of bands at 1730–1690 cm^{-1}, where COOH is expected to appear, is indicative of fully deprotonated btc^{3-} ligands in **1** and **3**.[43] The extensive hydrogen-bonding network present in the crystal structures is indicated through the δ- and γ-vibrational modes between 880 and 1350 cm^{-1} (see Experimental section).[44]

Crystal structure of $^{3}_{\infty}\{[Ni_3(\mu_3\text{-btc})_2(\mu_4\text{-btre})_2(\mu\text{-}H_2O)_2]\cdot{\sim}22H_2O\}$ 1

The nickel compound **1** features a trinuclear metal unit with two crystallographically different nickel sites.[45] The central Ni2 atom sits on an inversion center. Neighboring Ni1 and Ni2 atoms are bridged by two triazole groups and one aqua ligand. The coordination sphere of the two outer Ni1 atoms is concluded by three carboxyl oxygen atoms from three btc ligands. Each btre ligand connects four nickel atoms and each btc^{3-} ligand bridges between three symmetry related Ni1 atoms (Fig. 1a).

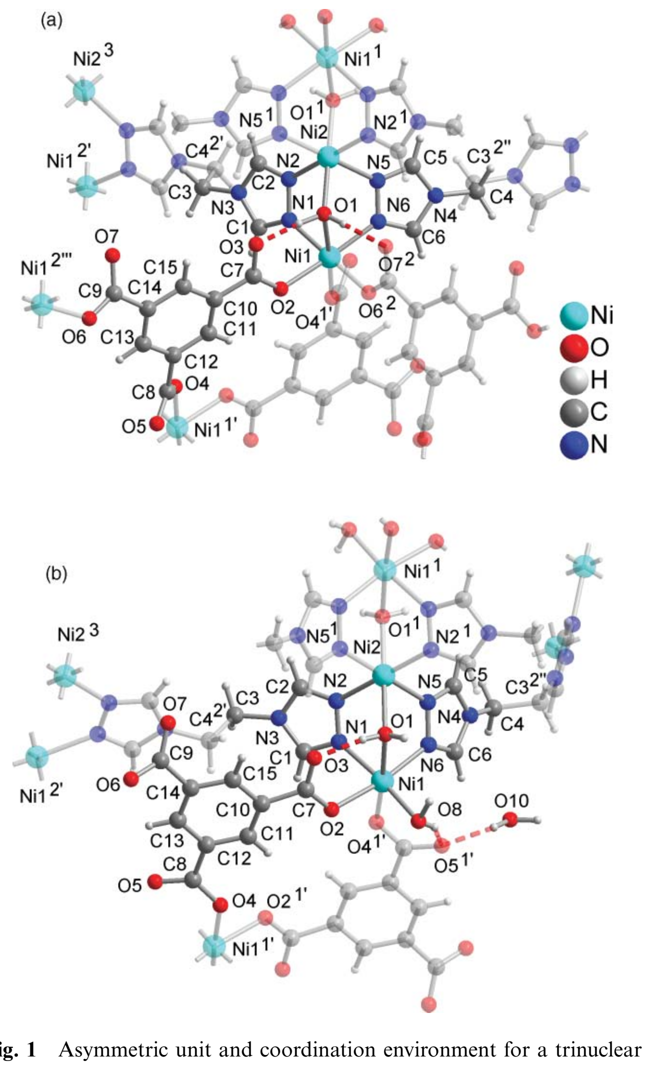

Fig. 1 Asymmetric unit and coordination environment for a trinuclear nickel unit in (a) **1** and (b) **2**. Ligands or ligand parts not belonging to the asymmetric unit are depicted semi-transparent. Selected distances and angles in Table 1. Hydrogen bonding interactions as red dashed lines (details see ESI†). Symmetry codes in **1**: 1 = $-x, -y, -z$; 1′ = $1 - x, -y, -z$; 2 = $x, -0.5 - y, 0.5 + z$; 2′ = $x, 0.5 - y, -0.5 + z$; 2″ = $x, 0.5 - y, 0.5 + z$; 2‴ = $x, -0.5 - y, -0.5 + z$; 3 = $-x, 0.5 + y, -0.5 - z$; in **2**: 1 = $-x, 1 - y, 1 - z$; 1′ = $1 - x, 1 - y, -z$; 2′ = $x, 1.5 - y, -0.5 + z$; 2″ = $x, 1.5 - y, 0.5 + z$; 3 = $-x, 0.5 + y, 0.5 - z$.

Table 1 Selected bond lengths (Å) and angles (°) in **1** and **2**[a]

	1	2
Ni1–O1	2.145(2)	2.177(9)
Ni1–O2	2.060(2)	2.092(7)
Ni1–O4$^{1'}$	2.005(2)	1.995(8)
Ni1–O6^{2}/O8 [b]	2.067(2)	2.009(9)
Ni1–N1	2.064(2)	2.066(9)
Ni1–N6	2.071(2)	2.082(8)
Ni2–O1	2.062(2)	2.112(7)
Ni2–N2	2.091(2)	2.060(8)
Ni2–N5	2.077(2)	2.100(9)
Ni1 · · · Ni2	3.3971(3)	3.460(1)
cis-O–Ni–O	86.2(1)–92.3(1)	87.1(3)–93.9(4)
O1–Ni1–O4$^{1'}$	177.0(1)	176.2(3)
cis-N1–Ni–O	84.0(1)–94.4(1)	84.2(3)–92.1(3)
N1–Ni1–O6^{2}/O8 [b]	176.0(1)	172.2(3)
cis-N6–Ni–O	83.5(1)–99.1(1)	83.8(3)–99.7(3)
N6–Ni1–O2	174.7(1)	171.8(3)
N1–Ni1–N6	92.0(1)	87.6(3)
cis-O1–Ni–N	85.2(1)–94.8(1)	83.8(3)–96.1(3)
N2–Ni2–N5	90.5(1)	89.5(3)
N2–Ni2–N5^{1}	89.5(1)	90.5(3)
Ni2–O1–Ni1	107.7(1)	107.6(3)

[a] Full angle list in ESI. Symmetry relations in **1**: 1 = $-x, -y, -z$; 1′ = $1 - x, -y, -z$; 2 = $x, -0.5 - y, 0.5 + z$; in **2**: 1 = $-x, 1 - y, 1 - z$; 1′ = $1 - x, 1 - y, 1 - z$. [b] O6^{2} in **1** and O8 in **2**.

The Ni1 atoms and the btc ligands alone form parallelepipedic 4,4 (4^2) nets parallel to the *bc*-plane (Fig. 2a). Also, the Ni atoms and the btre ligands form parallelepipedic 4,4 nets parallel to *bc* (Fig. 2b). Along the *a*-direction these nets alternate and connect with each other through the Ni atoms and aqua bridges (Fig. 2c).

The bridging action of the two different ligands in **1** gives rise to a 3D framework with large water-filled channels along *a* (Fig. 3). From structure refinement of the electron density in these channels, thermogravimetric analysis and the available channel volume (from PLATON) about 22 disordered water molecules of crystallization are estimated per Ni_3 formula unit. In the absence of the water of crystallization the potential solvent volume is 1621 Å^3 per unit cell volume of 3115.8 Å^3 (= 52%). With the expected volume for a hydrogen-bonded H_2O molecule of ~40 Å^3 this agrees with 44 H_2O molecules per unit cell (2 formula units) or 22 H_2O per Ni_3 formula unit. An experimental nitrogen adsorption study on an evacuated sample (after 3 d at 50 °C) indicated some minor porosity with a BET surface area of about 400 $m^2\ g^{-1}$.† This minor porosity is closer to the potential solvent volume calculated in compound **2** (see below) in the absence of the water of crystallization as 196 Å^3 (10% of the unit cell volume of 1937 Å^3).

Crystal structure of $^{3}_{\infty}\{[Ni_3(\mu_2\text{-btc})_2(\mu_4\text{-btre})_2(\mu\text{-}H_2O)_2(H_2O)_2]\cdot 4H_2O\}$ 2

The freeze-dried crystal product retains the trinuclear nickel unit with its bridging aqua and btre-ligands (Fig. 1b). The main difference between **1** and **2** in the Ni_3 unit is the replacement of one of the three coordinating btc^{3-} ligands on Ni1 in **1** by a terminal aqua ligand (O8) in **2**. In **2** the btc^{3-} ligand bridges only between two symmetry related Ni1 atoms. Hence, the Ni1 atoms and btc

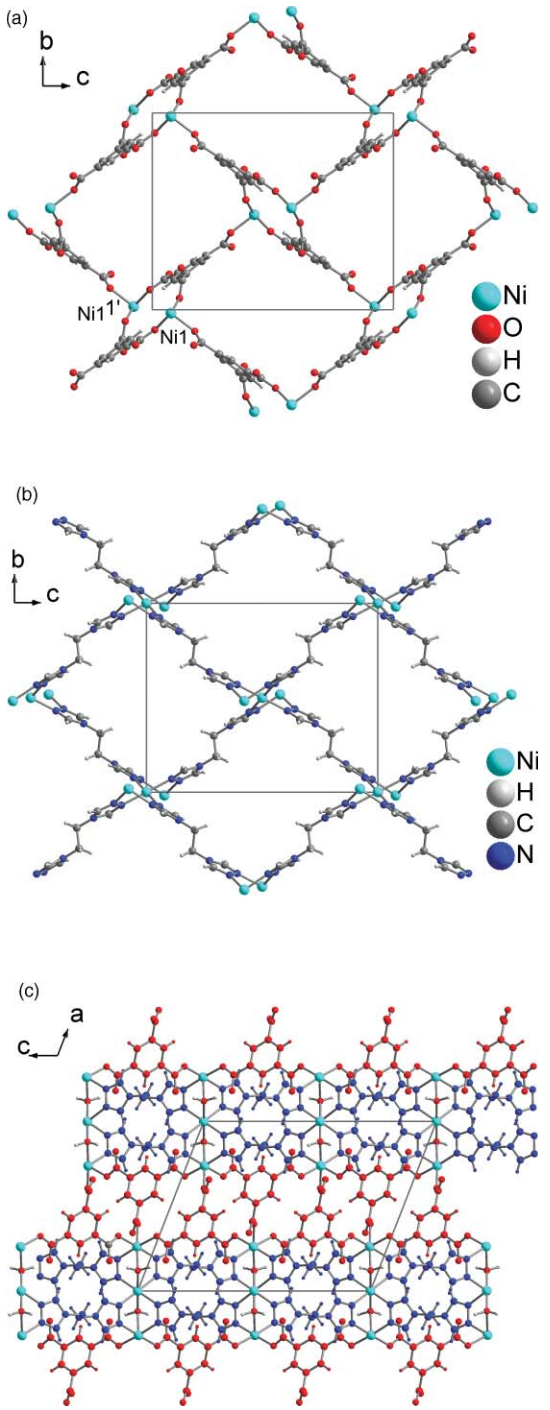

Fig. 2 Packing analysis for **1** by differentiation in individual (a) {Ni-btc}- and (b) {Ni-btre}-nets. (c) Alternation of the {Ni-btc}- and {Ni-btre}-nets. In (c) aqua ligands and all btc atoms are shown in red, all atoms of the btre ligands are given in blue, zinc atoms in light blue.

ligands alone form dinuclear units in **2** (Fig. 4a) instead of 2D nets as in **1**. The Ni atoms and the btre ligands still form 4,4 nets, albeit strongly distorted (Fig. 4b). The bridging action of the two different ligands in **2** results in a densely packed 3D-framework (Fig. 5) with only four enclathrated crystal water molecules per Ni_3 unit. Removal of the crystal water from **1** leads to a collapse of the framework along the *b*-axis, which shrinks to ~60%, together

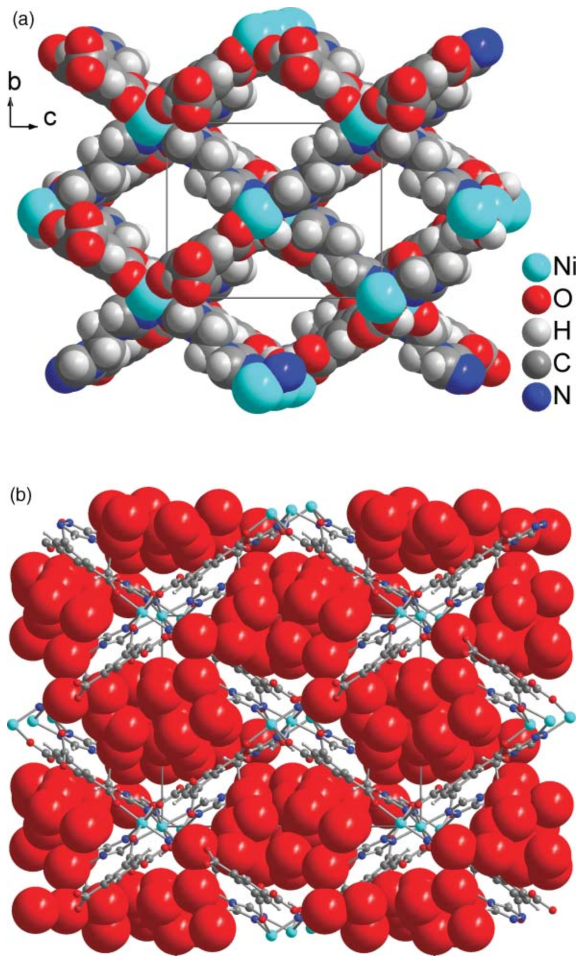

Fig. 3 Packing diagram for **1**; (a) space-filling drawing of the metal–ligand framework with water of crystallization in the channels omitted; (b) ball-and-stick drawing of the framework with water of crystallization in space-filling mode.

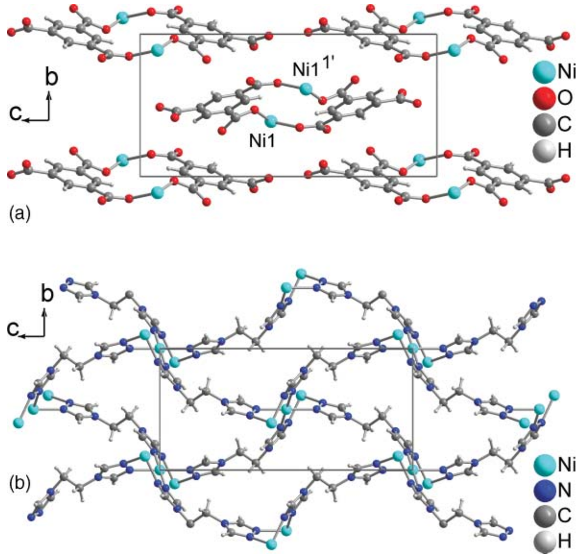

Fig. 4 Packing analysis for **2** by differentiation in individual (a) {Ni-btc}-units and (b) {Ni-btre} nets. Note the shortening of the *b*-axis to 61% in comparison to the *b*-axis of structure **1** in Fig. 2.

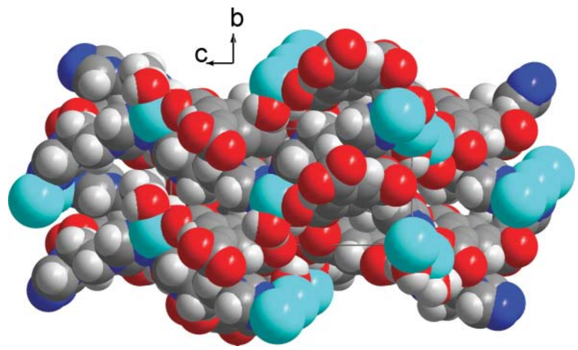

Fig. 5 Space-filling packing diagram for **2**.

with the unit cell volume, when going from **1** to **2**. The motion of units for **1** → **2** is evident upon comparison of Fig. 2a,b with Fig. 4a,b.

Crystal structure of $^{3}_{\infty}\{[Zn_3(\mu_4\text{-btc})_2(\mu_4\text{-btre})_2(H_2O)_2]\cdot 2H_2O\}$, 3

The zinc compound **3** features a trinuclear metal unit with three crystallographically different zinc atoms (Fig. 6a). Two neighboring zinc atoms are bridged by a triazole and a carboxylate group. The octahedral coordination sphere of the central Zn2 is concluded by two aqua ligands. Atom Zn1 is four-coordinate with two more oxygen atoms from carboxylate groups. Atom Zn3 becomes five-coordinate since one of the coordinating carboxylate groups is approaching a chelate formation. Each btre and each btc^{3-} ligand connect four zinc atoms (Fig. 6a).

The Zn atoms and the btc ligands alone form corrugated nets parallel to the {0 2 −4}-plane (Fig. 7a). The Zn2 atoms and the btre ligands form strands parallel to the *b*-axis (Fig. 7b).

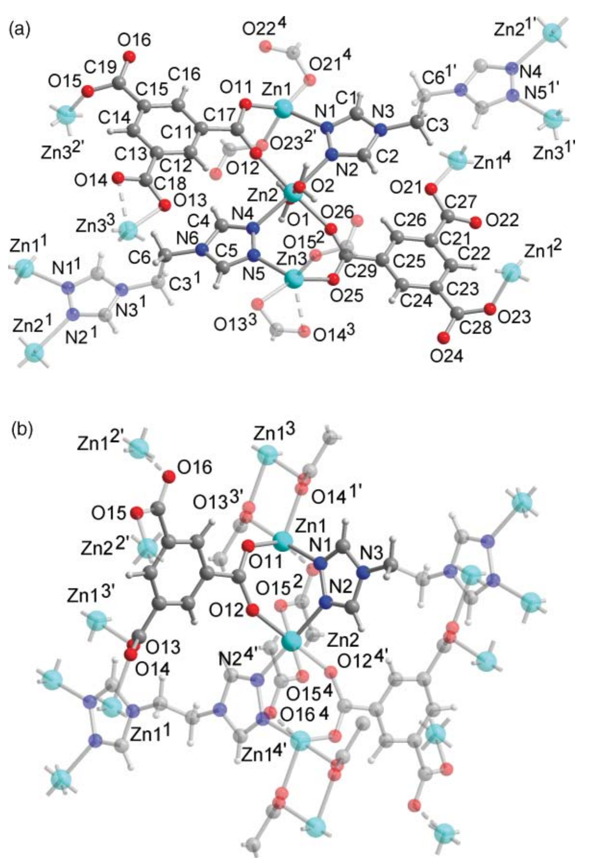

Fig. 6 Asymmetric unit and coordination environment for a trinuclear zinc unit in (a) **3** and (b) **4**. Ligands or ligand parts not belonging to the asymmetric unit are depicted semi-transparent. Selected distances and angles in Table 2. Symmetry codes in **3**: 1 = *x*, −1 + *y*, *z*; 1′ = *x*, 1 + *y*, *z*; 2 = −1 + *x*, *y*, *z*; 2′ = 1 + *x*, *y*, *z*; 3 = −*x*, 1 − *y*, −*z*; 4 = 1 − *x*, 3 − *y*, 1 − *z*; in **4**: 1 = *x*, *y*, 1 + *z*; 1′ = *x*, *y*, −1 + *z*; 2 = 1 + *x*, 1 + *y*, *z*; 2′ = −1 + *x*, −1 + *y*, *z*; 3 = 1 − *x*, −*y*, 1 − *z*; 3′ = 1 − *x*, −*y*, 2 − *z*; 4 = −*x*, −*y*, 2 − *z*; 4′ = 1 − *x*, 1 − *y*, 2 − *z*.

Table 2 Selected bond lengths (Å) and angles (°) in **3** and **4**[a]

	3[b]	**4**
Zn1–O11/Zn3–O25	1.918(2)/1.945(2)	1.970(2)
Zn1–O21^{4}/Zn3–O13^{3}	1.940(2)/2.104(2)	—
≡ Zn1–O14$^{1'}$ in **4**	—	2.138(2)
Zn1–O23$^{2'}$/Zn3–O15^{2}	2.023(2)/1.989(2)	—
≡ Zn1–O13$^{3'}$ in **4**	—	2.040(2)
Zn1–O16^{2} in **4**	—	2.299(2)
Zn1–N1/Zn3–N5	2.067(2)/2.068(2)	2.124(2)
Zn2–O1/Zn2–O2	2.058(2)/2.076(2)	—
≡ Zn2–O15^{2} in **4**	—	2.177(2)
Zn2–O12/Zn2–O26	2.143(2)/2.070(2)	2.063(2)
Zn2–N2/Zn2–N4	2.182(2)/2.146(2)	2.070(2)
–/Zn3–O14^{3}	–/2.233(2)	—
O11–Zn1–O21^{4}/O25–Zn3–O13^{3}	138.41(7)/150.98(7)	—
≡ O11–Zn1–O14$^{1'}$ in **4**	—	99.79(8)
O11–Zn1–O23$^{2'}$/O25–Zn3–O15^{2}	95.11(6)/97.90(6)	—
≡ O11–Zn1–O13$^{3'}$ in **4**	—	91.56(8)
O21^{4}–Zn1–O23$^{2'}$/O13^{3}–Zn3–O15^{2}	106.87(7)/95.04(6)	—
≡ O13$^{3'}$–Zn1–O14$^{1'}$ in **4**	—	84.54(8)
O11–Zn1–O16^{2}	—	146.56(8)
O13$^{3'}$–Zn1–O16^{2}	—	96.61(8)
O14$^{1'}$–Zn1–O16^{2}	—	113.22(8)
O11–Zn1–N1/O25–Zn3–N5	115.13(7)/109.55(7)	86.04(9)
O21^{4}–Zn1–N1/O13^{3}–Zn3–N5	91.21(7)/86.57(7)	—
≡ O14$^{1'}$–Zn1–N1 in **4**	—	91.91(8)
O23$^{2'}$–Zn1–N1/O15^{2}–Zn3–N5	108.34(7)/118.18(7)	—
≡ O13$^{3'}$–Zn1–N1 in **4**	—	175.33(9)
O16–Zn1–N1	—	87.57(9)
–/O13^{3}–Zn3–O14^{3}	–/60.25(6)	—
–/O15^{2}–Zn3–O14^{3}	–/96.33(7)	—
–/O25–Zn3–O14^{3}	–/92.47(6)	—
–/O14^{3}–Zn3–N5	–/134.58(7)	—
O1–Zn2–O2	176.43(6)	—
≡ O15^{2}–Zn2–O15^{4} in **4**	—	180.0
O1–Zn2–O12/O2–Zn2–O26	94.92(7)/91.52(7)	—
≡ O15^{2}–Zn2–O12 in **4**	—	80.53(8)
O1–Zn2–O26/O2–Zn2–O12	85.94(7)/87.51(7)	—
≡ O15^{4}–Zn2—O12 in **4**	—	99.47(8)
O12–Zn2–O26	177.50(6)	—
≡ O12–Zn2–O12$^{4'}$ in **4**	—	180.0
O1–Zn2–N2/O2–Zn2–N4	85.53(7)/90.74(7)	—
≡ O15^{2}–Zn2–N2 in **4**	—	86.45(9)
O2–Zn2–N2/O1–Zn2–N4	91.88(7)/91.97(7)	—
≡ O15^{4}–Zn2–N2 in **4**	—	93.55(9)
O12–Zn2–N2/O26–Zn2–N4	89.29(6)/94.53(7)	84.59(9)
O26–Zn2–N2/O12–Zn2–N4	88.44(7)/87.78(6)	—
≡ O12–Zn2 N2$^{4'}$–in **4**	—	95.41(9)
N2–Zn2–N4	175.98(6)	—
≡ N2–Zn2–N2$^{4'}$ in **4**	—	180.0

[a] Symmetry relations in **3**: 1 = *x*, −1 + *y*, *z*; 1′ = *x*, 1 + *y*, *z*; 2 = −1 + *x*, *y*, *z*; 2′ = 1 + *x*, *y*, *z*; 3 = −*x*, 1 − *y*, −*z*; 4 = 1 − *x*, 3 − *y*, 1 − *z*; in **4**: 1 = *x*, *y*, 1 + *z*; 1′ = *x*, *y*, −1 + *z*; 2 = 1 + *x*, 1 + *y*, *z*; 2′ = −1 + *x*, −1 + *y*, *z*; 3 = 1 − *x*, −*y*, 1 − *z*; 3′ = 1 − *x*, −*y*, 2 − *z*; 4 = −*x*, −*y*, 2 − *z*; 4′ = 1 − *x*, 1 − *y*, 2 − *z*. [b] Related bonds and angles are grouped together for comparison with **4** where Zn2 sits on an inversion center, hence Zn3 becomes Zn1 and the asymmetric unit is halved.

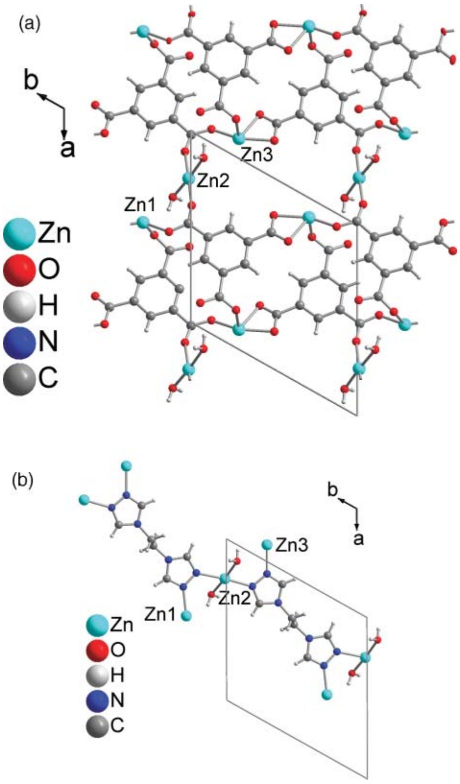

Fig. 7 Packing analysis for **3** by differentiation in individual (a) {Zn-btc}-nets and (b) {Zn2-btre}-strands.

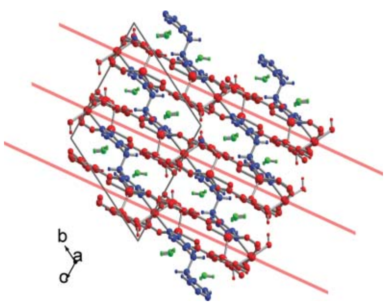

Fig. 8 Packing diagram for **3** viewed along the {0 2 −4}-planes (indicated in pink). For clarity aqua ligands and all atoms of the benzene tricarboxylate ligands are shown in red, all atoms of the bis(triazolyl)ethane ligands in blue, atoms of the water molecules of crystallization are depicted in green, zinc atoms in light blue.

The bridging action of the two different ligands in **3** gives rise to a 3D-framework with water-filled channels in-between the {0 2 −4}-planes (Fig. 8). Two hydrogen-bonded water molecules of crystallization are found per Zn3 formula unit. In the absence of the water of crystallization the potential solvent volume is 94 Å^3 per unit cell volume of 1394.1 Å^3 (= 7%) (calculated with PLATON). All hydrogen atoms of the aqua ligands and water of crystallization are engaged in normal hydrogen-bonding interactions (see ESI†).

Crystal structure of $^{3}_{\infty}\{[Zn_3(\mu_6\text{-btc})_2(\mu_4\text{-btre})_2]\cdot\sim0.67H_2O\}$, 4

The dehydrated product no longer has aqua ligands at the central zinc atom of the trinuclear unit. Instead, btc-carboxylate groups from the adjacent Zn-btc layers now occupy the positions of the former aqua ligands in **3** (Fig. 6a and b). These carboxylate groups also bridge between Zn1 and Zn2. Furthermore, two carboxylate groups now bridge between neighboring, symmetry related Zn1 atoms. In **4** every carboxylate group bridges two zinc atoms. Thus, the btc ligand connects six zinc atoms now. The Zn-btc substructure becomes a 3D framework (2D in **3**) (Fig. 9a). The Zn2 atoms and btre ligands still form strands (Fig. 9b). The overall packing is rather dense. Some residual electron density can be refined to ~2/3 of a crystal water molecule per Zn_3 unit. The crystal-to-crystal transition from **3** to **4** is a concerted motion of units which involves breakage and new formation of Zn–O bonds and which is difficult to follow in these 3D-frameworks. The bond reformation is due to the known lability of Zn–ligand bonds. When going from **3** with 2 Zn_3 to **4** with 1 Zn_3 fragments per unit cell the comparative volume is reduced from 1394.1 to 2 × 609.7 Å^3 or to 87%.

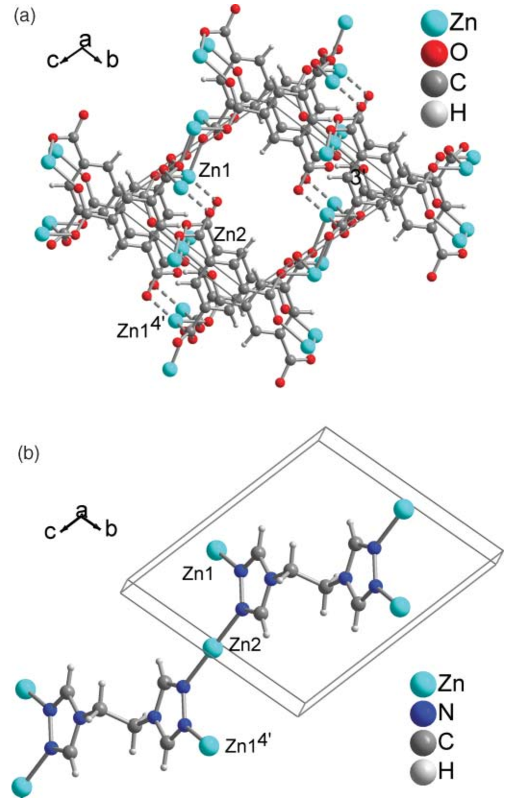

Fig. 9 Packing analysis for **4** by differentiation in individual (a) {Zn-btc}-nets and (b) {Zn2-btre}-strands.

Magnetic properties of 1 (air-dried sample)

The thermal dependence of $\chi_M T$ (χ_M being the magnetic susceptibility per mol of Ni_3) for the title complex in the temperature range 1.9–300 K is shown in Fig. 10. The value of $\chi_M T$ at room temperature (3.25 cm^3 mol^{-1} K) corresponds to what is expected for three non-interacting single-ion triplet states.[46] On cooling, the $\chi_M T$ value decreases to reach a plateau between 10 and 5 K, with values around 1.10 cm^3 mol^{-1} K (this corresponds to a $S = 1$ spin state, $g = 2.11$) and finally decreases to 0.88 cm^3 mol^{-1} K at 1.9 K. These features are typical for antiferromagnetically coupled high-spin Ni_3 systems with weak antiferromagnetic inter-trimer interactions or zero-field-splitting (zfs). This behavior leads to

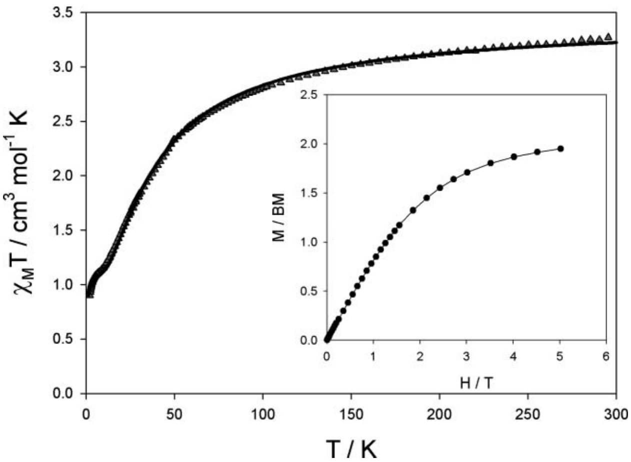

Fig. 10 Thermal dependence of the $\chi_M T$ for an air-dried sample of compound **1**. The solid line is the best fit to eqn (6), see text. The insert corresponds to the M *vs* H plot at 2 K.

a $S = 1$ ground state, that corresponds to the plateau reached between 5–10 K in the $\chi_M T$ *vs* T plot, also observed in the M *vs* H plot, shown in the insert of Fig. 10. For such a system the magnetic exchange interactions are usually described by the isotropic Hamiltonian (eqn (4))

$$\hat{H} = -J(\hat{S}_1\hat{S}_2 + \hat{S}_2\hat{S}_3) - j\hat{S}_1\hat{S}_3) \quad (4)$$

where J and j represent the exchange coupling constant between neighboring and terminal ions, respectively.[46] In the absence of a clear exchange-pathway between terminal ions j is taken as zero, and the Eigenvalues are then given by eqn (5)

$$E(S_A, S_T) = -\frac{J}{2}[S_T(S_T + 1) - S_A(S_A + 1)] \quad (5)$$

where S_A is the spin quantum number associated with the spins $S_1 + S_3$ and S_T is the total spin. S_A takes the values 2, 1 and 0, whereas S_T takes values from $|S_A + 1|$ to $|S_A - 1|$. The ground state is found to be $|S_A = 2, S_T = 1>$. The introduction of the Zeeman term and the application of Van Vleck's approach to these energy levels give the analytical expression for the susceptibility (eqn (6)):

$$\chi_M = \frac{N\beta^2 g^2}{k(T - \Theta)}\left(\frac{2 + 12x^2 + 2x^3 + 10x^4 + 28x^5}{3 + x + 8x^2 + 3x^3 + 5x^4 + 7x^5}\right) \quad (6)$$

N stands for Avogadro's number, g the Landé factor, β the Bohr magneton, k the Boltzman's constant and $x = e^{J/kT}$. At low temperatures an isolated trinuclear complex should follow the Curie law. But we have mentioned that below 5 K the $\chi_M T$ values for **1** lie below the theoretical values for a spin triplet. This suggests that other kinds of magnetic effect take place among the trinuclear units at low temperatures; these have been taken into account by the introduction of a Weiss-like parameter (Θ) in eqn (6). [A zfs of the $S = 1$ spin state would also lead to a decrease of the $\chi_M T$ values at low temperatures, however the determination of D from polycrystalline samples is not very accurate[47] and implies an important complication in the calculations, so we have considered this decrease in $\chi_M T$ as attributbale to intermolecular antiferromagnetic interactions and we give a maximum value.] Best least-squares fit of the magnetic susceptibility data of compound **1** to eqn (6) gave the parameters: $g = 2.14(1)$, $J = -13.88(8)$ cm^{-1}, $\theta = -0.34(2)$ K and $R = 0.9995$. The calculated curve matches very well the experimental data over the whole temperature range, as can be seen in Fig. 10. Antiferromagnetic interactions in N1,N2 triazole-bridged Ni(II) complexes have been previously observed with J-values that range from -16 to -22.2 cm^{-1}.[46] The J-value observed for **1** is not far from those previously reported, indicating that the substituents in the triazole ligands do not affect to a large extent the magnetic coupling among the Ni(II) ions.

Emission properties of 3

The zinc compound **3** shows a strong fluorescence emission at 423 nm upon excitation at 323 nm (Fig. 11). The benzene-1,3,5-tricarboxylic acid has no fluorescence and 1,2-bis(1,2,4-triazol-4-yl)ethane (btre) gives no fluorescence response at room temperature. Thus, zinc coordination of the btre ligand leads to a strong enhancement in fluorescence. An increase in fluorescence intensity is often seen in luminescence studies of zinc, cadmium and silver coordination polymers.[1,48,49]

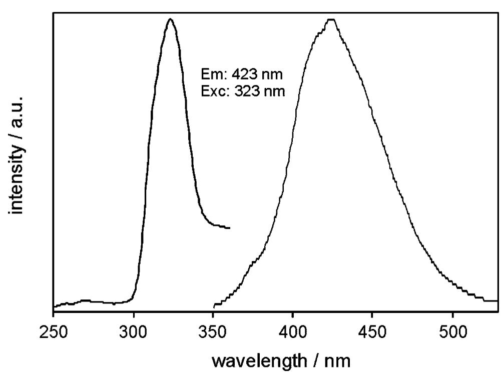

Fig. 11 Excitation and emission spectrum of compound **3**.

Conclusions

The ligand combination of 1,2-bis(1,2,4-triazol-4-yl)ethane (btre) and fully deprotonated benzene-1,3,5-tricarboxylate (btc^{3-}) leads to trinculear secondary building blocks with nickel and zinc cations within 3D metal–organic frameworks. The nickel atoms in the Ni_3 unit are antiferromagnetically coupled. Incorporated crystal water and also aqua ligands for Zn can largely be removed through freeze drying for the Ni and carefully controlled heating for the Zn compound to give the dehydrated products as single crystals in a solid-state single-crystal-to-single-crystal transition. The dehydration involves considerable restructuring of the framework with a decrease of the unit cell volume to 60% for Ni and Zn–O bond breakage and new formation for Zn. Zinc coordination to the btre ligand turns on a luminescence response upon UV excitation (not seen in the free ligand).

Experimental

Commercially available solvents, monoformylhydrazine, triethyl orthoformate, ethylenediamine, benzene-1,3,5-tricarboxylic acid (H_3btc), $Ni(NO_3)_2 \cdot 6H_2O$ and $Zn(NO_3)_2 \cdot 6H_2O$ were used without further purification. The ligand 1,2-bis(1,2,4-triazol-4-yl)ethane (btre) was prepared according to the method of Bayer *et al.*[50]

Dried methanol is used for the preparation of the btre ligand. Elemental analyses were performed on a VarioEL from Elementaranalysensysteme GmbH. Infrared spectra were recorded in the range 400–4000 cm^{-1} on a Bruker Optik IFS 25 spectrophotometer using KBr pellets. Thermogravimetric analysis was carried out in a simultaneous thermoanalysis apparatus STA 409C from Netzsch under nitrogen with a heating rate of 10 °C min^{-1} in the range 50 to 600 °C. The filled sample container was conditioned by first applying oil pump vacuum down to 1 bar for 5 min, then flushing with nitrogen, except for the TGA of compound **1**. A porosity measurement for a dried sample of **1** was carried out on Quantachrome Autosorb automated gas sorption system. Powder X-ray diffraction patterns were measured at ambient temperature using a STOE STADI-P with Debye-Scherrer geometry, Mo-Kα radiation ($\lambda = 0.7093$ Å), a Ge(111) monochromator with the samples in glass capillaries on a rotating probe head. Simulated powder patterns were based on single-crystal data and calculated using the STOE WinXPOW software package.[51] Theoretical porosity calculations for the potential solvent volume in the solvent-depleted structures were carried out with PLATON.[52] Emission spectra were measured on a Perkin-Elmer LS-55, $\lambda_{exc} =$ 323 nm, split widths (em, ex) 5.0 nm, scan speed 2 nm s^{-1}, solid sample at room temperature.

Magnetic susceptibility measurements on polycrystalline samples were carried out in the temperature range 1.9–300 K by means of a Quantum Design SQUID magnetometer operating at 1000 Oe ($T < 15$ K) and 10000 Oe ($T > 15$ K). Diamagnetic corrections of the constituent atoms were estimated from Pascal's constants as -430×10^{-6} cm^3 mol^{-1} for **1**. Experimental susceptibilities were also corrected for the temperature-independent paramagnetism [100×10^{-6} cm^3 mol^{-1} *per* Ni(II)] and the magnetization of the sample holder.

Syntheses

Di(μ-aqua)-bis(μ$_3$-benzene-1,3,5-tricarboxylato)-bis(μ$_4$-1,2-bis(1,2,4-triazol-4-yl)ethane)-trinickel(II) hydrate, $^3_\infty$\{[Ni$_3$(μ$_3$-btc)$_2$(μ$_4$-btre)$_2$(μ-H$_2$O)$_2$]·~22H$_2$O\}, (1). A mixture of $Ni(NO_3)_2 \cdot 6H_2O$ (145 mg, 0.50 mmol), H_3btc (105 mg, 0.50 mmol), triethylamine (210 μL, 1.5 mmol), btre (82 mg, 0.50 mmol) and water (15 mL) was stirred for 30 min at room temperature, transferred to a Teflon-lined stainless-steel autoclave and heated at 180 °C for 3 d. Then the autoclave was cooled to room temperature at a rate of 2.8 °C h^{-1}. A blue crystalline product was filtered off, washed with distilled water and dried in air (yield 180 mg, 86% based on Ni). Elemental analysis on air-dried compound: fully hydrated $C_{30}H_{70}Ni_3N_{12}O_{36}$ (1351.11) calcd C 26.67, H 5.22, N 12.44; loss of 5 H_2O $C_{30}H_{60}Ni_3N_{12}O_{31}$ (1260.94) calcd C 28.57, H 4.80, N 13.33; loss of 10 H_2O $C_{30}H_{50}Ni_3N_{12}O_{26}$ (1170.87) calcd C 30.77, H 4.30, N 14.36; found: C 28.12, H 4.81, N 13.16%; IR (KBr) 3423(br, ν(O–H)), 3125(w), 1611(s, $\nu_{asym}CO_2$), 1560(s, $\nu_{asym}CO_2$), 1436(s, $\nu_{sym}CO_2$), 1361(s, $\nu_{sym}CO_2$), 1223(m, δ(OH···O)), 1173(w), 1083(s), 1034(m), 1007(w), 888(m, γ(OH···O)), 802(m), 713(s), 644(s), 460(w) cm^{-1}.

Diaqua-bis(μ$_4$-benzene-1,3,5-tricarboxylato)-(μ$_4$-1,2-bis(1,2,4-triazol-4-yl)ethane)-trizinc(II) dihydrate, $^3_\infty$\{[Zn$_3$(μ$_4$-btc)$_2$(μ$_4$-btre)(H$_2$O)$_2$]·2H$_2$O\}, (3). A mixture of $Zn(NO_3)_2 \cdot 6H_2O$ (297 mg, 1.00 mmol), H_3btc (210 mg, 1.00 mmol), triethylamine (420 μL, 3.00 mmol), btre (164 mg, 1.00 mmol) and water (10 mL) was stirred for 30 min at room temperature, transferred to a Teflon-lined stainless-steel autoclave and heated at 180 °C for 3 d. Then the autoclave was cooled to room temperature at a rate of 2.8 °C h^{-1}. A colorless crystalline product was filtered off, washed with distilled water and dried in air (yield 200 mg, 71% based on Zn). Elemental analysis $C_{24}H_{22}N_6O_{16}Zn_3$ (846.59) calcd C 34.05, H 2.62, N 9.93; found: C 34.13, H 2.66, N 9.94%; IR (KBr) 3448(w, ν(O-H)), 3119(w), 1627(s, $\nu_{asym}CO_2$), 1580(s, $\nu_{asym}CO_2$), 1442(s, $\nu_{sym}CO_2$), 1362(s, $\nu_{sym}CO_2$), 1204(m, δ(OH···O)), 1170(w), 1078(m), 1046(m), 1006(w), 911(m, δ(OH···O)), 820(w), 760(s), 728(s), 689(m), 650(s), 553(w), 451(w) cm^{-1}.

X-Ray crystallography

Suitable single crystals were carefully selected under a polarizing microscope.

Data Collection. Bruker AXS with APEXII CCD area-detector, Mo-Kα radiation ($\lambda = 0.71073$ Å), graphite monochromator, double-pass method ω-scan, data collection and cell refinement with SMART,[53] data reduction with SAINT,[53] experimental absorption correction with SADABS.[54]

Structure analysis and refinement. The structure was solved by direct methods (SHELXS-97);[55] refinement was done by full-matrix least squares on F^2 using the SHELXL-97 program suite.[55] All non-hydrogen positions were found and refined with anisotropic temperature factors. Hydrogen atoms on the aromatic rings and the carbon atoms were placed at calculated positions with an appropriate riding model (AFIX 43 for aromatic CH, AFIX 23 for CH_2) and an isotropic temperature factor of $U_{eq}(H) =$ 1.2 $U_{eq}(CH, CH_2)$. In **1** the hydrogen atoms on the crystal water molecules were neither found nor refined. The crystal water in **1** is only given by its oxygen atoms. Some of the disordered oxygen atoms of the water of crystallization were refined isotropically with "anti-bumping" restraints (BUMP −0.02). If the sum of occupancies of the two atoms is less than 1.1, no restraint is generated. The occupancies of all 17 crystal water O atom positions were refined simultaneously until the very last refinement cycles. Occupancies refined between about 0.15, 0.30, 0.60, 0.90 and 1.000. In the last refinement cycles these occupancies were then kept fixed at these rounded values, which summed to 22 O atoms per Ni_3 formula unit. Any short inter D···A contacts (< 2.5 Å) between crystal water O atoms which are still listed by CheckCif were viewed as a time-averaged disordered water structure. This disorder is also a manifestation of high mobility and dynamic behavior among the crystal solvent molecules. At a given moment only one out of two partly occupied O atoms will really be present at their position. Hence, if some of these partly occupied refined O atoms are removed, such that the remaining O···O contacts are longer than 2.7–2.8 Å, these remaining O atom positions would then represent a real picture of the hydrogen-bonded crystal water phase at this moment.[56] The crystal-to-crystal transformation upon dehydration from **1** to **2** is not perfect as evidenced by the crystal of **2** diffracting only to $2\theta = 39.8°$. Still, all atoms in **2** could be unequivocally found and refined, including the H atoms on the aqua ligands. Only the core atoms, that is nickel and its directly bound atoms, were refined anisotropically in **2**. The remaining non-hydrogen atoms were only refined isotropically because of the otherwise too low reflection-to-parameter ratio.

Table 3 Crystal data and structure refinement for **1** to **4**

Compound	**1**	**2**	**3**	**4**
Empirical formula	$C_{30}H_{70}N_{12}Ni_3O_{36}$ [e]	$C_{30}H_{38}N_{12}Ni_3O_{20}$	$C_{24}H_{22}N_6O_{16}Zn_3$	$C_{24}H_{15.33}N_6O_{12.66}Zn_3$
M/g mol^{-1}	1351.11 [e]	1062.85	846.59	786.58
Crystal size/mm	0.21 × 0.18 × 0.06	0.43 × 0.22 × 0.03	0.40 × 0.40 × 0.30	0.35 × 0.18 × 0.03
2θ range/°	7.1–51.3	3.2–39.8	3.8–53.2	4.6–55.7
h; k; l range	−14, +16; −16, +12; ±21	±13; ±7; ±17	±14; ±15; ±15	±11; ±11; ±12
Crystal system	Monoclinic	Monoclinic	Triclinic	Triclinic
Space group	$P2_1/c$	$P2_1/c$	$P\bar{1}$	$P\bar{1}$
a/Å	13.9111(2)	13.7399(9)	11.8109(2)	8.5489(3)
b/Å	13.5328(2)	8.2320(5)	11.9995(2)	8.9997(4)
c/Å	17.7634(3)	18.8439(13)	12.4175(3)	9.6016(7)
α/°	90	90	109.047(1)	100.890(3)
β/°	111.292(1)	114.636(4)	105.825(1)	104.282(3)
γ/°	90	90	110.960(1)	115.281(2)
V/Å^3	3115.81(8)	1937.4(2)	1394.08(5)	609.73(6)
Z	2	2	2	1
D_{calcd}/g cm^{-3}	1.393	1.822	2.017	2.140
F (000)	1324	1092	852	392
μ/mm^{-1}	0.993	1.545	2.655	3.017
Max/min transmiss.	0.9428/0.8193	0.9551/0.5564	0.451/0.360	0.9149/0.4182
Refl. collected (R_{int})	16499 (0.0240)	8884 (0.0613)	26451 (0.0371)	16073 (0.0529)
Indep. reflections	5855	1772	5757	2858
Obs. refl.. [$I > 2\sigma(I)$]	5066	1360	4726	2292
Parameters refined	407	192	466	217
Max./min. $\Delta\rho$/e Å^{-3} [a]	0.827/–0.593	1.155/–0.510	0.466/–0.633	0.617/–0.475
R_1/wR_2 [$I > 2\sigma(I)$] [b]	0.0398/0.1076	0.0658/0.1562	0.0274/0.0733	0.0318/0.0726
R_1/wR_2 (all reflect.) [b]	0.0473/0.1125	0.0894/0.1739	0.0382/0.0793	0.0464/0.0779
Goodness-of-fit on F^2 [c]	1.039	1.018	1.040	1.027
Weight. scheme w; a/b [d]	0.0647/3.5335	0.0885/18.3368	0.0440/0.0306	0.0398/0.3825

[a] Largest difference peak and hole. [b] $R_1 = [\sum(\|F_o| - |F_c\|)/\sum|F_o|]$; $wR_2 = [\sum[w(F_o^2 - F_c^2)^2]/\sum[w(F_o^2)^2]]^{1/2}$. [c] Goodness-of-fit $= [\sum[w(F_o^2 - F_c^2)^2]/(n - p)]^{1/2}$. [d] $w = 1/[\sigma^2(F_o^2) + (aP)^2 + bP]$ where $P = (\max(F_o^2 \text{ or } 0) + 2F_c^2)/3$. [e] 44 H atoms on crystal water not located but included in formula and formula mass.

Hydrogen atoms on the crystal water molecules were found but had to remain fixed (AFIX 1) upon subsequent refinement. In **3** the hydrogen atoms of the water molecules were found and refined with $U_{eq}(H) = 1.5\ U_{eq}(O)$. Simulated X-ray powder diffractograms from the single-crystal data were matched with measured X-ray powder diffractograms for **1**, **2** and **3** to verify the representative nature of the single crystal with respect to the bulk material. Some decomposition was apparent for **1** (see ESI†). Graphics were obtained with DIAMOND.[57] Crystal data and details on the structure refinement are given in Table 3.

Acknowledgements

The work is supported by KAAD and by DFG grant Ja466/14–1. We acknowledge the Servicio General de Medidas Magnéticas of Universidad de La Laguna for the magnetic measurements facilities.

References

1 C. Janiak, *Dalton Trans.*, 2003, 2781–2804.

2 Xiang Lin, Junhua Jia, P. Hubberstey, M. Schröder and N. R. Champness, *CrystEngComm*, 2007, **9**, 438–448; C. L. Cahill, D. T. de Lill and M. Frisch, *CrystEngComm*, 2007, **9**, 15–26; D. Maspoch, D. Ruiz-Molina and J. Veciana, *Chem. Soc. Rev.*, 2007, **36**, 770–818; A. Y. Robin and K. M. Fromm, *Coord. Chem. Rev.*, 2006, **250**, 2127–2157; Chun-Long Chen, Bei-Sheng Kang and Cheng-Yong Su, *Aust. J. Chem*, 2006, **59**, 3–18; S. Kitagawa, S.-I. Noro and T. Nakamura, *Chem. Commun.*, 2006, 701–707; C. J. Kepert, *Chem. Commun.*, 2006, 695–700; Youfu Zhou, Maochun Hong and Xintao Wu, *Chem. Commun.*, 2006, 135–143; N. R. Champness, *Dalton Trans.*, 2006, 877–880; U. Mueller, M. Schubert, F. Teich, H. Puetter, K. Schierle-Arndt and J. Pastré, *J. Mater, Chem.*, 2006, **16**, 626–636; S. L. James, *Chem. Soc. Rev.*, 2003, **32**, 276.

3 Recent examples: Dingxian Jia, Aimei Zhu, Jie Deng, Yong Zhang and Jie Dai, *Dalton Trans.*, 2007, 2083–2086; N. Sato and S.-I. Nishikiori, *Dalton Trans.*, 2007, 1115–1119; G. S. Matouzenko, M. Perrin, B. Le Guennic, C. Genre, G. Molnar, A. Bousseksou and S. A. Borshch, *Dalton Trans.*, 2007, 934–942; J. E. Beves, E. C. Constable, C. E. Housecroft, C. J. Kepert and D. J. Price, *CrystEngComm*, 2007, **9**, 456–459; P. Thuéry, *CrystEngComm*, 2007, **9**, 460–462; Xiaojuan Gu and Dongfeng Xue, *CrystEngComm*, 2007, **9**, 471–477; S. M. Krishnan, N. M. Patel, W. R. Knapp, R. M. Supkowski and R. L. LaDuca, *CrystEngComm*, 2007, **9**, 503–514; Jun-Wei Ye, Jia Wang, Jing-Ying Zhang, Ping Zhang and Yue Wang, *CrystEngComm*, 2007, **9**, 515–523; R. Carballo, B. Covelo, E. Garcia-Martinez, A. B. Lago and E. M. Vázquez-López, *Z. Anorg, Allg. Chem.*, 2007, **633**, 780–782; K. Mueller-Buschbaum and Y. Mokaddem, *Z. Anorg, Allg. Chem.*, 2007, **633**, 521–523; W. R. Knapp, J. G. Thomas, D. P. Martin, M. A. Braverman, R. J. Trovitch and R. L. LaDuca, *Z. Anorg, Allg. Chem.*, 2007, **633**, 575–581; A. Roth, A. Buchholz and W. Plass, *Z. Anorg, Allg. Chem.*, 2007, **633**, 383–392; Qian Chu, Ling-Yan Kong, T. Okamura, H. Kawaguchi, Wen-Li Meng, Wei-Yin Sun and N. Ueyama, *Z. Anorg, Allg. Chem.*, 2007, **633**, 326–331; K. Abu-Shandi, H. Winkler and C. Janiak, *Z. Anorg, Allg. Chem.*, 2006, **632**, 629–633; K. Abu-Shandi, H. Winkler, H. Paulsen, R. Glaum, Biao Wu and C. Janiak, *Z. Anorg, Allg. Chem.*, 2005, **631**, 2705–2714; K. Abu-Shandi and C. Janiak, *Z. Naturforsch., B*, 2005, **60**, 1250–1254.

4 K. Biradha, M. Sarkar and L. Rajput, *Chem. Commun.*, 2006, 4169–4179; Bao-Hui Ye, Ming-Liang Tong and Xiao-Ming Chen, *Coord. Chem. Rev.*, 2005, **249**, 545–565.

5 Recent examples of mixed-ligand coordination polymers: B. Wisser, Yirong Lu and C. Janiak, *Z. Anorg. Allg. Chem.*, 2007, **633**, 1189–1192; S. C. Manna, K.-I. Okamoto, E. Zangrando and N. R. Chaudhuri, *CrystEngComm*, 2007, **9**, 199–292; Zhen-Feng Chen, Shu-Feng Zhang, Hai-Sheng Luo, B. F. Abrahams and Hong Liang, *CrystEngComm*,

2007, **9**, 27–29; A. Pichon, C. M. Fierro, M. Nieuwenhuyzen and S. James, *CrystEngComm*, 2007, **9**, 449–451; J. Pasán, J. Sanchiz, F. Lloret, M. Julve and C. Ruiz-Pérez, *CrystEngComm*, 2007, **9**, 478–487; M. D. Stephenson and M. J. Hardie, *Dalton Trans.*, 2006, 3407–3417; R. Carballo, B. Covelo, E. M. Vázquez-López, E. García-Martínez, A. Castiñeiras and C. Janiak, *Z. Anorg, Allg. Chem.*, 2005, **631**, 2006–2010.
6 Jie-Peng Zhang and Xiao-Ming Chen, *Chem. Commun.*, 2006, 1689–1699; A. Rodriguez-Dieguez, A. Salinas-Castillo, S. Galli, N. Masciocchi, J. M. Gutierrez-Zorrilla, P. Vitoria and E. Colacio, *Dalton Trans.*, 2007, 1821–1828.
7 Cambridge Structure Database search, CSD Version 5.28 (November 2006) with 2 updates (January 2007, May 2007).
8 A. Majumder, S. Shit, C. R. Choudhury, S. R. Batten, G. Pilet, D. Luneau, N. Daro, J.-P. Sutter, N. Chattopadhyay and S. Mitra, *Inorg. Chim. Acta*, 2005, **358**, 3855.
9 M. J. Plater, M. R. St, J. Foreman, E. Coronado, C. J. Gomez-Garcia and A. M. Z. Slawin, *J. Chem. Soc., Dalton Trans.*, 1999, 4209.
10 M. J. Plater, M. R. St, J. Foreman, R. A. Howie, J. M. S. Skakle, E. Coronado, C. J. Gomez-Garcia, T. Gelbrich and M. B. Hursthouse, *Inorg. Chim. Acta*, 2001, **319**, 159.
11 M. Du, X.-J. Jiang and X.-J. Zhao, *Inorg. Chem.*, 2006, **45**, 3998.
12 T. J. Prior and M. J. Rosseinsky, *CrystEngComm*, 2000, **2**, 128.
13 P. Wang, C. N. Moorefield, M. Panzer and G. R. Newkome, *Chem. Commun.*, 2005, 465; P.-K. Chen, Y.-X. Che and J.-M. Zheng, *Jiegou Huaxue*, 2006, **25**, 1427; R. Pech and J. Pickardt, *Acta Crystallogr., Sect.C: Cryst. Struct. Commun.*, 1988, **44**, 992.
14 Q. Wang, M.-J. Wu, X.-G. Wang and X.-J. Zhao, *Acta Crystallogr., Sect. E: Struct. Rep. Online*, 2006, **62**, m2496; Y.-F. Zhou, B.-Y. Lou, D.-Q. Yuan, Y.-Q. Xu F.-L. and M.-C. Hong, *Inorg. Chim. Acta*, 2005, **358**, 3057; O. M. Yaghi, G. Li and H. Li, *Chem. Mater.*, 1997, **9**, 1074.
15 X. Shi, G. Zhu, Q. Fang, G. Wu, Ge Tian, R. Wang, D. Zhang, M. Xue and S. Qiu, *Eur. J. Inorg, Chem.*, 2004, 185.
16 M. Riou-Cavellec, C. Albinet, J.-M. Greneche and G. Ferey, *J. Mater. Chem.*, 2001, **11**, 3166.
17 B.-B. Ding, Y.-Q. Weng, Z.-W. Mao, C.-K. Lam, X.-M. Chen and B.-H. Ye, *Inorg. Chem.*, 2005, **44**, 8836.
18 O. M. Yaghi, H. Li and T. L. Groy, *J. Am. Chem. Soc.*, 1996, **118**, 9096; O. M. Yaghi, G. Li and H. Li, *Nature (London)*, 1995, **378**, 703.
19 C. Daiguebonne, A. Deluzet, M. Camara, K. Boubekeur, N. Audebrand, Y. Gerault, C. Baux and O. Guillou, *Cryst. Growth Des.*, 2003, **3**, 1015; K.-Y. Choi, K. M. Chun and I.-H. Suh, *Polyhedron*, 2001, **20**, 57; A. Michaelides, S. Skoulika, V. Kiritsis, C. Raptopoulou and A. Terzis, *J. Chem Res.*, 1997, **204**, 1344.
20 W. Chen, X.-N. Tan, Y.-M. Li, J.-M. Zheng and Y.-X. Che, *Wuji Huaxue Xuebao*, 2005, **21**, 1901; D. Bradshaw, T. J. Prior, E. J. Cussen, J. B. Claridge and M. J. Rosseinsky, *J. Am Chem. Soc.*, 2004, **126**, 6106; X. Zhao, B. Xiao, A. J. Fletcher, K. M. Thomas, D. Bradshaw and M. J. Rosseinsky, *Science*, 2004, **306**, 1012; T. J. Prior, D. Bradshaw, S. J. Teat and M. J. Rosseinsky, *Chem. Commun.*, 2003, 500; T.-B. Lu, H. Xiang, R. L. Luck, L. Jiang, Z.-W. Mao and L.-N. Ji, *New J. Chem.*, 2002, **26**, 969; H. J. Choi, T. S. Lee and M. P. Suh, *J. Inclusion, Phenom. Macrocyclic Chem.*, 2001, **41**, 155; T.-B. Lu, H. Xiang, R. L. Luck, Z.-W. Mao, D. Wang, C. Chen and L.-N. Ji, *CrystEngComm*, 2001, **3**, 168; C. J. Kepert, T. J. Prior and M. J. Rosseinsky, *J. Am, Chem. Soc.*, 2000, **122**, 5158; C. J. Kepert and M. J. Rosseinsky, *Chem. Commun.*, 1998, 31; H. J. Choi and M. P. Suh, *J. Am, Chem. Soc.*, 1998, **120**, 10622.
21 S. Liang, H. Wang, Z. Wang and J.-Y. Han, *Acta Crystallogr., Sect. E: Struct. Rep. Online*, 2006, **62**, m3014.
22 K. E. Holmes, P. F. Kelly and M. R. J. Elsegood, *Dalton Trans.*, 2004, 3488.
23 Q.-W. Zhang and G.-X. Wang, *Z. Kristallogr.-New Cryst. Struct.*, 2006, **221**, 101; J. W. Ko, K. S. Min and M. P. Suh, *Inorg. Chem.*, 2002, **41**, 2151; H. Oshio and H. Ichida, *J. Phys, Chem.*, 1995, **99**, 3294.
24 J. Zhang, Y.-B. Chen, S.-M. Chen, Z.-J. Li, J.-K. Cheng and Y.-G. Yao, *Inorg. Chem.*, 2006, **45**, 3161; G. Wu, X. Shi, Q. Fang, G. Tian, L. Wang, G. Zhu, A. W. Addison, Y. Wei and S. Qiu, *Inorg. Chem. Commun.*, 2003, **6**, 402; X. Li, D. Sun, R. Cao, Y. Sun, Y. Wang, W. Bi, S. Gao and M. Hong, *Inorg. Chem. Commun.*, 2003, **6**, 908.
25 S. Qin, S. Lu, Y. Ke, J. Li, S. Zhou, X. Wu and W. Du, *Cryst. Res. Technol.*, 2006, **41**, 98; S. Qin, S. Lu, Y. Ke, J. Li, S. Zhou, X. Wu and W. Du, *Zh. Strukt. Khim.*, 2004, **45**, 566.
26 G. Smith, A. N. Reddy, K. A. Byriel and C. H. L. Kennard, *J. Chem, Soc., Dalton Trans.*, 1995, 3565.
27 B. Gomez-Lor, E. Gutierrez-Puebla, M. Iglesias, M. A. Monge, C. Ruiz-Valero and N. Snejko, *Chem. Mater.*, 2005, **17**, 2568.
28 X.-F. Xue, Y.-X. Che, L. Xue and J.-M. Zheng, *Jiegou Huaxue*, 2005, **24**, 1181.
29 Y. Garcia, P. J. van Koningsbruggen, G. Bravic, P. Guionneau, D. Chasseau, G. L. Cascarano, J. Moscovici, K. Lambert, A. Michalowicz and O. Kahn, *Inorg. Chem.*, 1997, **36**, 6357; Jia-Cheng Liu, De-Gang Fu, Jin-Zhong Zhuang, Chun-Ying Duan and Xiao-Zeng You, *J. Chem. Soc., Dalton Trans.*, 1999, 2337; P. J. Hagrman, C. Bridges, J. E. Greedan and J. Zubieta, *J. Chem, Soc., Dalton Trans.*, 1999, 2901; K. Drabent and Z. Ciunik, *Chem. Commun.*, 2001, 1254; Y. Garcia, J. Moscovici, A. Michalowicz, V. Ksenofontov, G. Levchenko, G. Bravic, D. Chasseau and P. Gütlich, *Chem.–Eur. J.*, 2002, **8**, 4992; Y. Garcia, P. J. van Koningsbruggen, G. Bravic, D. Chasseau and O. Kahn, *Eur. J. Inorg, Chem.*, 2003, 356; Bing Liu, Guo-Cong Guo and Jin-Shun Huang, *J. Solid, State Chem.*, 2006, **179**, 3136; Bin Ding, Yong Quan Huang, Yuan Yuan Liu, Wei Shi and Peng Cheng, *Inorg. Chem. Commun.*, 2007, **10**, 7.
30 Hyunsoo Park, D. M. Moureau and J. B. Parise, *Chem. Mater.*, 2006, **18**, 525.
31 Long Yi, Bin Ding, Bin Zhao, Peng Cheng, Dai-Zheng Liao, Shi-Ping Yan and Zong-Hui Jiang, *Inorg. Chem.*, 2004, **43**, 33; Yong-Quan Huang, Bin Ding, Hai-Bin Song, Bin Zhao, Peng Ren, Peng Cheng, Hong-Gen Wang, Dai-Zheng Liao and Shi-Ping Yan, *Chem. Commun.*, 2006, 4906.
32 G. Vos, A. J. de Kok and G. C. Verschoor, *Z. Naturforsch., B: Chem. Sci.*, 1981, **36**, 809; H. Schmidbaur, A. Mair, G. Müller, J. Lachmann and S. Gamper, *Z. Naturforsch., B: Chem. Sci.*, 1991, **46**, 912; O. Castillo, U. Garcia-Couceiro, A. Luque, J. P. Garcia-Teran and P. Roman, *Acta Crystallogr., Sect. E: Struct. Rep. Online*, 2004, **60**, m9; Liu Xuan-Wen, *Acta Crystallogr., Sect. E: Struct. Rep. Online*, 2005, **61**, m1777; P. Nockemann, F. Schulz, D. Naumann and G. Meyer, *Z. Anorg, Allg. Chem.*, 2005, **631**, 649; Bin Ding, Long Yi, Ying Wang, Peng Cheng, Dai-Zheng Liao, Shi-Ping Yan, Zong-Hui Jiang, Hai-Bin Song and Hong-Gen Wang, *Dalton Trans.*, 2006, 665; Bing Liu, Ling Xu, Guo-Cong Guo and Jin-Shun Huang, *J. Mol. Struct.*, 2006, **825**, 79; E. Aznar, S. Ferrer, J. Borras, F. Lloret, M. Liu-Gonzalez, H. Rodriguez-Prieto and S. Garcia-Granda, *Eur. J. Inorg. Chem.*, 2006, 5115.
33 A. B. Lysenko, E. V. Govor, H. Krautscheid and K. V. Domasevitch, *Dalton Trans.*, 2006, 3772; A. B. Lysenko, E. V. Govor and K. V. Domasevitch, *Inorg. Chim. Acta*, 2007, **360**, 55.
34 $[Mn(NCS)_2(\mu\text{-btr-}\kappa N1,N1')(H_2O)_2]$: M. Biagini-Cingi, A. M. Manotti-Lanfredi, F. Ugozzoli, J. G. Haasnoot and J. Reedijk, *Gazz. Chim. Ital.*, 1994, **124**, 509.
35 $\{[Mn(NCS)(\mu\text{-btr-}\kappa N1,N1')(\text{btr-}\kappa N1)_2(H_2O)]NCS\}$: C. L. Zilverentant, W. L. Driessen, J. G. Haasnoot, J. J. A. Kolnaar and J. Reedijk, *Inorg. Chim. Acta*, 1998, **282**, 257.
36 $[Co(NCS)_2(\mu\text{-btr-}\kappa N1,N1')_2]$: W. Vreugdenhil, S. Gorter, J. G. Haasnoot and J. Reedijk, *Polyhedron*, 1985, **4**, 1769.
37 $[Mn(\mu\text{-}N_3\text{-}\kappa N1,N3)_2(\text{btr-}\kappa N1)_2]$: Xin-Yi Wang, Lu Wang, Zhe-Ming Wang, Gang Su and Song Gao, *Chem. Mater.*, 2005, **17**, 6369.
38 $[Fe(NCS)_2(\mu\text{-btr-}\kappa N1,N1')_2]$: W. Vreugdenhil, J. H. van Diemen, R. A. G. de Graaff, J. G. Haasnoot, J. Reedijk, A. M. van der Kraan, O. Kahn and J. Zarembowitch, *Polyhedron*, 1990, **9**, 2971.
39 Baolong Li, Zheng Xu, Zhengbai Cao, Liming Zhu and Kaibei Yu, *Transition Met. Chem.*, 1999, **24**, 622; Baolong Li, Jianzhong Zou, Chunying Duan, Yongjiang Liu, Xianwen Wei and Zheng Xu, *Acta Crystallogr., Sect. C: Cryst. Struct. Commun.*, 1999, **55**, 165; Baolong Li, Baozong Li, Xia Zhu, Liming Zhu and Yong Zhang, *Acta Crystallogr., Sect. C: Cryst. Struct. Commun.*, 2003, **59**, m350; Xia Zhu, Bao-Zong Li, Jun-Hui Zhou, Bao-Long Li and Yong Zhang, *Acta Crystallogr., Sect. C: Cryst. Struct. Commun.*, 2004, **60**, m191; Junhui Zhou, Xia Zhu, Yunnan Zhang, Yong Zhang and Baolong Li, *Inorg. Chem. Commun.*, 2004, **7**, 949; Baolong Li, Baozong Li, Xia Zhu, Xinghua Lu and Yong Zhang, *J. Coord, Chem.*, 2004, **57**, 1361; Baolong Li, Xia Zhu, Junhui Zhou, Yanfen Peng and Yong Zhang, *Polyhedron*, 2004, **23**, 3133.
40 Y. Garcia, G. Bravic, C. Gieck, D. Chasseau, W. Tremel and P. Gütlich, *Inorg. Chem.*, 2005, **44**, 9723.
41 Y. Garcia, P. J. van Koningsbruggen, H. Kooijman, A. L. Spek, J. G. Haasnoot and O. Kahn, *Eur. J. Inorg. Chem.*, 2000, 307.
42 Recent examples of crystal-to-crystal transformations in coordination polymers: A. Kondo, H. Noguchi, S. Ohnishi, H. Kajiro, A. Tohdoh, Y. Hattori, W.-C. Xu, H. Tanaka, H. Kanoh and K. Kaneko, *Nano Lett.*, 2006, **6**, 2581; D. Armentano, G. De Munno, T. F. Mastropietro, M. Julve and F. Lloret, *J. Am, Chem. Soc.*, 2005, **127**, 10778; A. K. Sah and T. Tanase, *Chem. Commun.*, 2005, 5980; Jian-Ping Ma,

Yu-Bin Dong, Ru-Qi Huang, M. D. Smith and Cheng-Yong Su, *Inorg. Chem.*, 2005, **44**, 6143; Ming-Hua Zeng, Xiao-Long Feng and Xiao-Ming Chen, *Dalton Trans.*, 2004, 2217; Chunhua Hu and U. Englert, *Angew. Chem., Int. Ed.*, 2005, **44**, 2281.

43 W. Brzyska and P. Sadowski, *Pol. J. Chem.*, 1987, **61**, 273; W. Brzyska and W. Wolodkiewicz, *Pol. J. Chem*, 1986, **60**, 697; K. Wieghardt, *J. Chem. Soc., Dalton Trans.*, 1973, 2548; L. J. Bellamy, *The Infrared Spectra of Complex Molecules*Wiley, New York, 1958.

44 F. A. A. Paz and J. Klinowski, *Inorg. Chem.*, 2004, **43**, 3882.

45 Cf. [{Ni(acac)$_2$}$_3$]:L. Wolf and E. Butter, *Z. Anorg. Allg. Chem.*, 1965, **339**, 191; G. J. Bullen, R. Mason and P. Pauling, *Inorg. Chem.*, 1965, **4**, 456.

46 B. Ding, L. Yi, W. Z. Shen, P. Cheng, D. Z. Liao, S. P. Yan and Z. H. Jiang, *J. Mol, Struct.*, 2006, **784**, 138; F. J. Rietmeijer, G. A. van Albada, R. A. G. de Graaff, J. G. Haasnoot and J. Reedijk, *Inorg. Chem.*, 1985, **24**, 3597; G. A. van Albada, R. A. G. de Graaff, J. G. Haasnoot and J. Reedijk, *Inorg. Chem.*, 1984, **23**, 1404.

47 O. Kahn, *Molecular Magnetism*, VCH, New York, Weinheim and Cambridge, 1993.

48 Shao-Liang Zheng and Xiao-Ming Chen, *Aust. J. Chem.*, 2004, **57**, 703.

49 B. Paul, B. Zimmermann, K. M. Fromm and C. Janiak, *Z. Anorg, Allg. Chem.*, 2004, **630**, 1650.

50 H. O. Bayer, R. S. Cook and W. C. von Meyer, *U. S. Patent*, 3 821 376, 1974.

51 *STOE WinXPOW Version 1.10*, STOE & Cie GmbH, Darmstadt, Germany, 2002.

52 A. L. Spek, *Acta Crystallogr., Sect. A*, 1990, **46**, C34; A. L. Spek, *PLATON–A Multipurpose Crystallographic Tool*, Utrecht University, The Netherlands, 2006; L. J. Farrugia, *PLATON Version 31-05-07; Windows implementation*, University of Glasgow, UK, 1995–2006.

53 *SMART, Data Collection Program for the CCD Area-Detector System; SAINT, Data Reduction and Frame Integration Program for the CCD Area-Detector System*, Bruker Analytical X-ray Systems, Madison, Wisconsin, USA, 1997.

54 G. Sheldrick, *Program SADABS: Area-detector absorption correction*, University of Göttingen, Germany, 1996.

55 G. M. Sheldrick, *SHELXS-97, SHELXL-97, Programs for Crystal Structure Analysis*, University of Göttingen, Germany, 1997.

56 C. Janiak, T. G. Scharmann and S. A. Mason, *J. Am, Chem. Soc.*, 2002, **124**, 14010–14011; C. Janiak, T. G. Scharmann, H. Hemling, D. Lentz and J. Pickardt, *Chem. Ber.*, 1995, **128**, 234–244.

57 K. Brandenburg, *Diamond (Version 3.1e), Crystal and Molecular Structure Visualization*, Crystal Impact–K. Brandenburg & H. Putz Gbr, Bonn, Germany 2007.

